Preprint
UCRL-JC-135735

High-Energy Electron, Positron, Ion and Nuclear Spectroscopy in Ultra-Intense Laser-Solid Experiments on the Petawatt

M. Roth, T. E. Cowan, A. W. Hunt, J. Johnson, C. Brown, W. Fountain, S. Hatchett, E. A. Henry, M. H. Key, T. Kuehl, T. Parnell, D. M. Pennington, M. D. Perry, T. C. Sangster, M. Christl, M. Singh, R. Snavely, M. Stoyer, Y. Takahashi, and S. C. Wilks

U.S. Department of Energy
Lawrence Livermore National Laboratory

This article was submitted to
First International Conference on Inertial Fusion Sciences and Applications
Bordeaux, France
September 12-17, 1999

September 16, 1999

High-Energy Electron, Positron, Ion and Nuclear Spectroscopy in Ultra-Intense Laser-Solid Experiments on the Petawatt

M. Roth[1,2], T.E. Cowan[2], A.W. Hunt[3], J. Johnson[4], C. Brown[2], W. Fountain[4], S. Hatchett[2], E.A. Henry[2], M.H. Key[2], T. Kuehl[1], T. Parnell[4], D.M. Pennington[2], M.D. Perry[2], T.C. Sangster[2], M. Christl[4], M. Singh[2], R. Snavely[2], M. Stoyer[2], Y. Takahashi[5] and S.C. Wilks[2]

[1]Gesellschaft für Schwerionenforschung, Darmstadt, Germany
[2] Lawrence Livermore National Laboratory, Livermore, CA, USA 94550
[3] Harvard University, Cambridge, MA, USA
[4] George C. Marshall Space Flight Center, Huntsville, AL, USA 35899
[5] University of Alabama, Huntsville, AL, USA 35899

Abstract

The LLNL Petawatt Laser has achieved focussed intensities up to 6×20 W/cm^2, which has opened a new, higher energy regime of relativistic laser-plasma interactions in which the quiver energies of the target electrons exceed the energy thresholds for many nuclear phenomena. We will describe recent experiments in which we have observed electrons accelerated to 100 MeV, photo-nuclear fission, and positron-electron pair creation.

Introduction

The generation of highly relativistic laser plasmas has become possible by using high power, chirped-pulse amplification lasers. Beyond the test of the fast ignition concept, these plasmas offer the possibility of very short pulse, high-energy electron and secondary radiation sources. The results presented in this report were obtained at the Petawatt Laser [1] at Lawrence Livermore National Laboratory. The Petawatt uses one arm of the NOVA laser to amplify a frequency-chirped pulse to kJ energies before temporal compression to ~450 fs. The peak power is well in excess of 1000 TW, and the beam can be focussed to a <10μm spot, with intensities of up to 6×10^{20} W/cm^2. At these intensities the electromagnetic fields at the laser focus are $E > 10^{13}$ V/m, and $B > 10^5$ Tesla and the motion of the electrons in the target plasma is fully relativistic. The cycle-averaged oscillation or "quiver" energy of the electrons,

$$\overline{E} = mc^2\left[1 + 2U_P/mc^2\right]^{1/2} \quad (1)$$

can exceed several MeV, where $U_P = 9.33 \times 10^{-14}\ I\ (W/cm^2)\lambda^2\ (\mu m)$ is the non-relativistic ponderomotive potential. The resulting distribution of electron energies in the target is predicted to resemble a Maxwellian [2], with mean energy given by Eq.1, and it extends far beyond the threshold for which nuclear effects become important. On the face of the solid targets used in these experiments a plasma was generated by a pre-pulse at 2 or 10 ns before the main pulse and with an amplitude tunable over 10^{-4} to 10^{-1} of the peak energy. The plasma served as a medium to self-focus the laser to increase the ponderomotive energy, and to produce electrons of even higher energy. The interaction of the electrons with the solid target produces high energy Bremsstrahlung, positron-electron pairs, and photo-nuclear reactions in the target material.

1. High-energy particle spectroscopy at the petawatt

To characterize the high-energy particles expelled from the target, we have fielded two compact, permanent magnet spectrometers [3,4] as shown in *Fig. 1*.

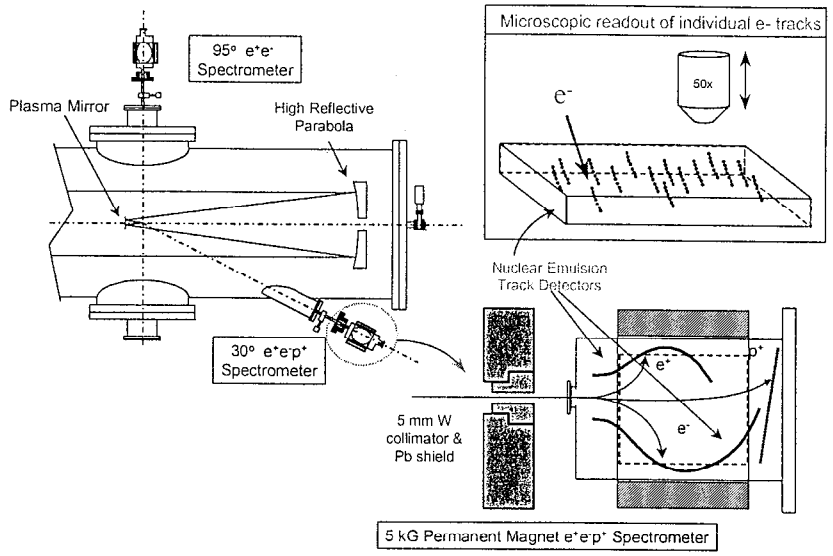

Fig1.: Schematic of the Petawatt target chamber and electron spectrometers. The laser beam enters from the left, is reflected from the parabola to a secondary plasma mirror, and reflected onto the target chamber center. The two spectrometers measure electrons (0.2 – 140 MeV), positrons (0.2 – 40 MeV) and ions (2 – 100 MeV) emitted at 30°and ~95° from the target.

The spectrometers detect electrons, positrons and ions at energies between a few hundred keV and 100 MeV. They are mounted at 30°and 95° with respect to the laser beam direction. The particles are recorded in nuclear emulsion track detectors, which are positioned such that the particle angle of incidence is a constant value of 10° throughout the dispersion plane. The emulsions consists of two layers of 50 μm thick, fine-grained silver bromide emulsion coated on the front and back surface of a 500 μm polystyrene strip. Microscopic examination of the developed emulsion strips allows clear identification of charged particle tracks and distinguishes electrons emitted from the target by virtue of the density of exposed grains along the track, the angle of incidence, and the transverse position along the emulsion strip. A second emulsion strip in each spectrometer is orientated to detect positrons within the energy range of 0.2 to 40 MeV and an additional detector strip was added later in the experiments to detect protons and heavy ions.

The analysis of the tracks in the nuclear emulsion allows single particle detection without being overwhelmed by the blinding x-ray flash from the laser plasma. Tracks of protons and heavy ions can be distinguished from those caused by positrons due to their higher specific energy deposition, which causes a thicker track in the emulsion. The spectrum of the particles is obtained by counting the number of individual tracks and converting the track densities to absolute differential cross sections. The energy distribution (i.e. position versus energy) was calculated by ray-tracing and confirmed by measurements performed at the LLNL electron linac. At a certain particle density threshold it is not possible to count single particles, because of the overlap of the individual tracks. Adding an x-ray film in front of the emulsion and analyzing the optical density in that film extends the sensitive range of the detector system.

The particle energy derived by the deflection in the magnetic field is in excellent agreement with the particle energy measured by the range in our multilayer detector.
(Energy calculated with TRIM - Codë)

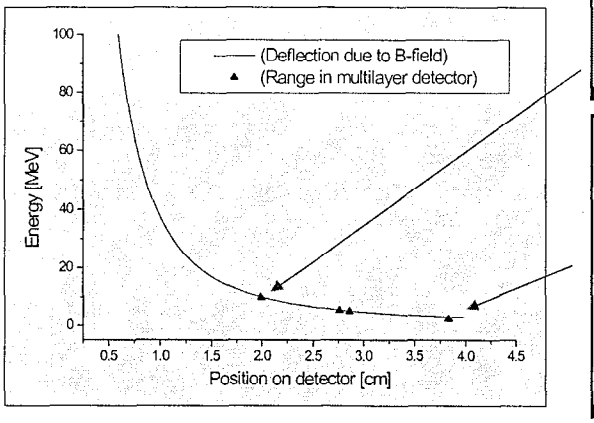

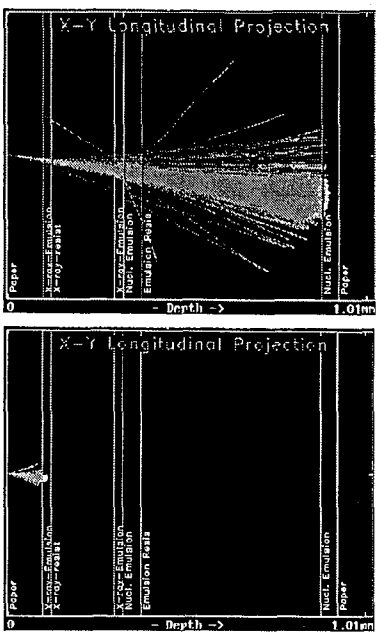

Figure 2: The energy needed to penetrate a certain depth in the multi-layer detector is compared to the position of the first appearance of the tracks on the respective film strip. As shown, there is an excellent agreement between the two methods.

The use of an x-ray film with a sensitive layer at the front and back side in combination with the two active layers of the nuclear emulsion and light protecting paper effectively represents an energy discriminating multi-layer detector. While the magnetic field of the spectrometer separates the momentum, the penetration depth of the particles in this detector reveals the energy signature of the particles. For a known particle species (e.g. protons), comparing the penetration depth of the particle with its momentum given by the position on the detector strip results in an additional and independent calibration method. The calibration of the spectrometer used energetic protons from the laser target. With the known thickness and chemical composition of all the different layers in the detector, the energy loss and range of the proton could be calculated. The calculations revealed a high sensitivity of the proton range in the strip detector. The energy obtained by the penetration of subsequent layers was then compared with the position of the first appearance of tracks in the respective layer. As shown in *Figure 2.*, there is an excellent agreement between the two calibration methods.

2. Laser-driven nuclear Fission and photo-nuclear reactions

Energetic electrons directed into the target are causing a substantial amount of hard Brems-strahlung x-rays in high-z target materials. Bremsstrahlung photons above the threshold for photo-nuclear reactions contribute to photo-neutron emission from the gold and copper and, if sufficiently intense, produce long-lived activities in the target [3,5,6]. After the laser shots, the targets were transported to a shielded high purity germanium gamma-ray spectrometer for time resolved measurements of the residual nuclear activation gamma rays produced by the laser shot. In one shot we encased 1.2g of ^{238}U within the copper sample holder. After this shot we observed a large collection of additional gamma lines, including several that were previously detected from photo-neutron reactions in the Au and Cu target material. An important aspect of this measurement is that we accumulated gamma-ray energy spectra in narrow time intervals following the shot. This allows us to identify many short- lived reaction products by both their gamma-ray line energy and their characteristic half-life. For example, by lifetime measurements of the 511 keV positron annihilation gamma-ray line observed after

the shot, we were able to identify the presence of the positron emitters, ^{64}Cu (12.7 h) and ^{62}Cu (9.7 m) produced by ^{65}Cu(γ,n)^{64}Cu and ^{63}Cu(γ.n)^{62}Cu reactions. The time-

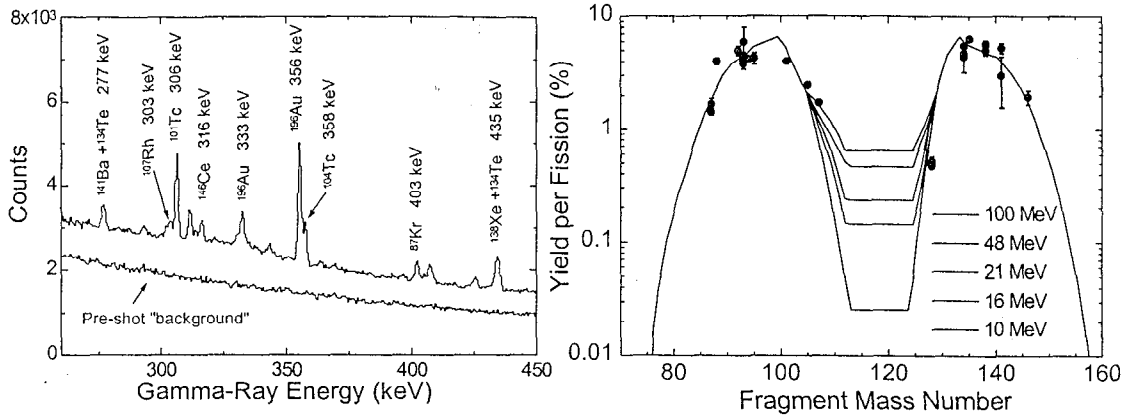

Fig3.: (left) Spectrum of nuclear de-excitation gamma-rays emitted from target assembly during 4 hours after Petawatt shot. (right) Yield of fission fragments identified by gamma spectroscopy. The ^{238}U characteristic,"double-humped" mass distribution is clearly visible.

resolved gamma-ray analysis was necessary to identify decay products from the photo-induced fission of ^{238}U [7]. The nuclides we have identified by their gamma-ray line energies and half lives include ^{87,88}Kr, ^{92,93}Sr, ^{93,94,95}Y, ^{101,104}Tc, ^{105}Ru, ^{107}Rh, ^{128}Sb, ^{128}Sn, ^{134}Te, ^{135}I, ^{138}Xe, ^{138}Cs, ^{141}Ba and ^{146}Ce. The data were compared to previous measurements [8] of yields for specific nuclides from photo-fission of ^{238}U with accelerator based Bremsstrahlung beams. As shown in *Fig. 3*, the mass distribution of the fission products lie upon the usual double-humped distribution caused by the large deformation of the ^{238}U parent. The total yield in this experiment was estimated to be (1.8±0.2)x 10^{7} photo-fission events, ^{238}U(γ,f). To provide information regarding the energy distribution of Bremsstrahlung photons produced by the plasma electrons over the range of ~5 to 20 MeV, photo-fission and photoneutron reactions can be used due to their different gamma-ray threshold energies. Taken together, the ^{238}U(γ,f),^{197}Au(γ,n) and ^{63,65}Cu(γ,n) reactions span a large range of effective nuclear excitation energies and hence provide good sensitivity for directly measuring the slope and total intensity of the Bremsstrahlung energy spectrum in the range of 5 to 20 MeV.

3. Positron emission and electron acceleration

3.1. Positron emission

The nuclear track emulsion technique presented above appears to be ideally suited for the detection of such rare events as the production of positrons, because of its intrinsic single-particle detection sensitivity, and because of the relative immunity of emulsions to the high-energy x-ray flux generated in relativistic laser plasmas. The yield of positron-electron pairs in our experiments is expected to be of order 10^{-4} of the electron yield in the energy range 5-10 MeV. The sparse nature of the positron data required a complete microscopic scanning of the entire emulsion strip, with critical attention paid to the quality and characteristics of each track to avoid spurious misidentification of scattered background events. Previously, we found that the observed positron yield was consistent with pair production of Bremsstrahlung photons in thick targets [5]. Fig.4 shows the positron distribution for a thin 125 μm Au target. The number of recorded positrons clearly exceeds the expected yield based on a fast-electron Bremsstrahlung mechanism. We are presently investigating whether this may be consistent with the direct production of positrons in electron-ion collisions in the relativistic plasma.

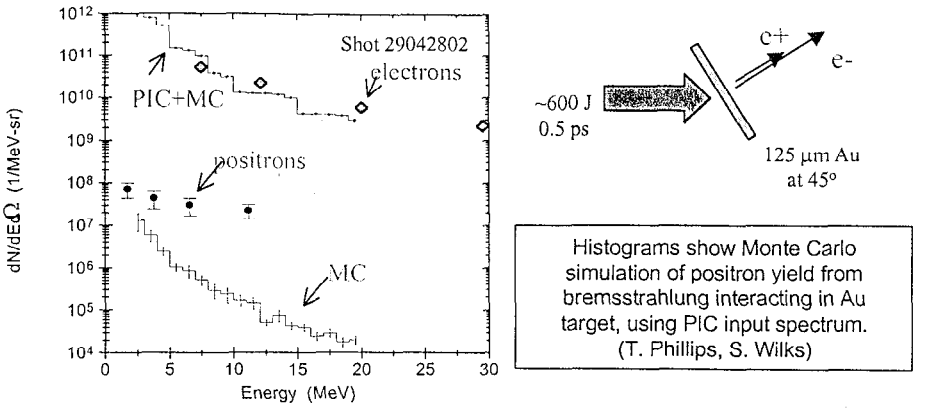

Fig4: Measurement of positron emission in 125 μm Au target Petawatt shot. The measured yield is in excess of the expected one based purely on Bremsstrahlung mechanism.

3.2. Electron acceleration

High energy electrons have been detected with energies up to 100 MeV which are predominantly localized in filaments in a strongly forward-peaked direction, but with poor reproducibililty. Electrons with energies in the few MeV range are distributed more homogenously, but show an interesting and not yet fully understood spectral behavior (see *Fig.5*).

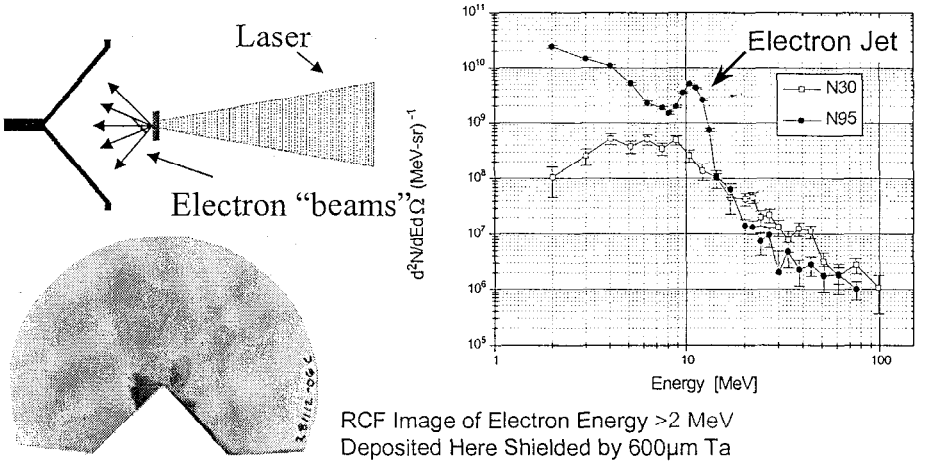

Fig 5: (left) experimental setup and image of the spatial distribution of electron from the target.(right) spectral electron distribution observed in many Petawatt shots reveal a jet like behaviour.

The overall flux of electrons derived from the optical density and calibrated by measurements of single particle tracks in the nuclear emulsion is in excellent agreement with the measured radiation dose deposited in our large solid-angle radiochromatic film detector [9], calibrated with an electron beam from an accelerator. The spectral distribution of the electrons is characterized by a lower portion, up to 20 MeV, which is consistent with the expected Maxwellian distribution having a mean energy of ~3MeV, predicted from Eq.1 and the presence of a high energy tail out to 100 MeV. This tail as well as the observation of a nearly monoenergetic beam-like structures indicates a more complicated laser-target interaction. In the energy range below 10 MeV, the measured electron energy spectra show a strong structured pattern.

4. Ion acceleration

At the high energy end of the positron strip single particle tracks of different size and depth could be detected. Assuming these tracks were caused by protons expelled from the target, the

spectrometer was modified in order to detect positive charged particles of high magnetic rigidity. A third detector, based on a combination of x-ray film and the nuclear emulsion was

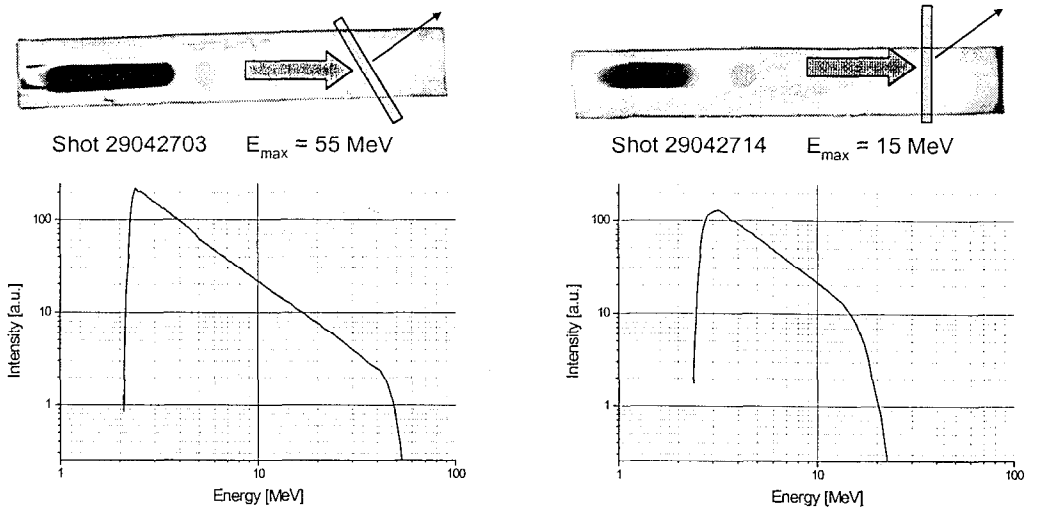

Fig.6: Pictures of the optical density of the nuclear emulsion and respective spectral distribution of the proton beams with respect to the orientation to the target rear-surface. The small black arrow in the left pictures denotes the direction towards the spectrometer.

placed at the end of the spectrometer (see *Fig.1*).The analysis of the data obtained during the last Petawatt shot series revealed a much larger amount of high energy protons than previously observed in other experiments. The corresponding energy spectrum shows protons up to 50 MeV with a distinct dependence on the orientation towards the target back-surface. The analysis of these data is not yet finished and will be published elsewhere. It is noteworthy, that the energy of protons perpendicular to the rear-surface of the target is significantly higher than at 45° angle. The existence of an intense proton beam could be also an important aspect in interpreting the measured neutron yield due to the opening of new (p,n) reaction channels in the target.

Work performed under the auspices of the U.S. Dept. of Energy by the Lawrence Livermore National Laboratory under Contract W-7405-Eng-48.

References

1 Perry, M. D.,Stuart B.C., Pennington D., Tietbohl G., Britten J.A.,Brown C., Herman S., Miller J., Powell H. T., Vergino M., Yanovsky V., *Optics Letters* **24**,160 (1999)

2 Wilks S. C., Kruer W. L., Tabak M. and Langdon A. B., *Phys. Rev. Lett.* **69**, p. 1383, (1992)

3 Cowan T. E. et al., "High Energy Electron Emission and Laser-Assisted Nuclear Transmutation in Petawatt Laser-Solid Interactions*", Proc. of the Int.l Conference on Lasers '97, J.J. Carroll & T.A. Goldman, eds., STS Press, McLean Va),* pp. 882-889 (1998)

4 Cowan T. E. et al., "Design and performance of a magnetic electron and positron spectrometer using nuclear emulsion track detection", to be published

5 Cowan T. E. et al, Laser Part. Beams **17**, 4 (1999)

6 Key, M.H.; Cable, M.D.; Cowan, T.E.; Estabrook, K.G.; Hammel, B.A.; Hatchett, S.P.; Henry, E.A.; Hinkel, D.E.; Kilkenny, J.D.; Koch, J.A.; Kruer, W.L.; Langdon, A.B.; Lasinski, B.F.; Lee, R.W.; MacGowan, B.J.; MacKinnon, A.; Moody, J.D.; Moran, M.J.; Offenberger, A.A.; Pennington, D.M.; Perry, M.D.; Phillips, T.J.; Sangster, T.C.; Singh, M.S.; Stoyer, M.A.; Tabak, M.; Tietbohl, G.L.; Tsukamoto, M.; Wharton, K.; Wilks, S.C. et al., Phys Plasmas **5**, 1966 (1998)

7 Cowen T. E., Hunt A. W. Phillip T. J., et al. , submitted to PRL

8 Kahane S. and Wolf A., Phys. Rev. **C32**, p.1944 (1985)

[9] Snafely R. to be published